

Isotope constraints on particulate nitrogen source and dynamics in the upper water column of the oligotrophic South China Sea

Shuh-Ji Kao,^{1,2} Jin-Yu Terence Yang,² Kon-Kee Liu,³ Minhan Dai,² Wen-Chen Chou,⁴ Hui-Ling Lin,⁵ and Haojia Ren⁶

Received 1 April 2011; revised 23 April 2012; accepted 2 May 2012; published 14 June 2012.

[1] Particulate nitrogen (PN) dynamics in the oligotrophic northern South China Sea (around the SouthEast Asian Time-series Study (SEATS) station) was explored by examining the isotopic compositions of suspended PN in the top 200 m over 3 years and sinking PN collected by sediment traps. The PN inventory (IPN) in the upper 100 m is larger than in the lower 100 m, exhibiting stronger seasonality. Both layers reveal significant seasonality in mean $\delta^{15}\text{N}_{\text{PN}}$, yet, the mean in the upper 100 m (2.0 to 5.3‰) is consistently smaller than that in the lower 100 m, implying the occurrence of vertical biological fractionation and/or an addition of ^{15}N -depleted N from the atmosphere. The $\delta^{15}\text{N}_{\text{PN}}$ surges in winter, when the mixed layer is deeper, indicate an intensified nitrate supply from thermocline, during which relatively stronger downward transfer efficiency was inferred by a small IPN gradient. The largest vertical gradient in IPN appeared during intermonsoon periods, corresponding with weak vertical mixing, low $\delta^{15}\text{N}_{\text{PN}}$, and high N^* values. N fixation is likely the cause for the intermonsoon $\delta^{15}\text{N}_{\text{PN}}$ lows. The $\delta^{15}\text{N}_{\text{PN}}$ values of trapped material at 374 m and 447 m range from 3.3 to 7.3‰ with a flux-weighted mean of 5.6‰ resembling the $\delta^{15}\text{NO}_3$ of upwelled sources. By using a mass-isotope balance model under the assumption of no atmospheric N deposition, we obtained an N fixation input of $\sim 20 \pm 26 \text{ mmol N m}^{-2} \text{ yr}^{-1}$. This value accounts for only ~ 5 – 10% of the new production on an annual basis.

Citation: Kao, S.-J., J.-Y. Terence Yang, K.-K. Liu, M. Dai, W.-C. Chou, H.-L. Lin, and H. Ren (2012), Isotope constraints on particulate nitrogen source and dynamics in the upper water column of the oligotrophic South China Sea, *Global Biogeochem. Cycles*, 26, GB2033, doi:10.1029/2011GB004091.

1. Introduction

[2] Nitrogen fixation has long been perceived as a dominant allochthonous source of newly fixed nitrogen to the ocean [Karl *et al.*, 1997; Montoya *et al.*, 2004]. The input of newly fixed nitrogen is one of the primary controls on the oceanic autotrophic productivity and organic matter sinking fluxes, thereby affecting the biological pump, which is

intimately coupled with the climate system through its modulation on the atmospheric CO_2 [Altabet *et al.*, 2002; Falkowski, 1997]. Yet the nitrogen dynamics in the surface ocean associated with nitrogen fixation are still neither well understood nor well quantified [Capone *et al.*, 1997], because nitrogen fixation is episodic and patchy and poses severe obstacles to direct observations [Mahaffey *et al.*, 2005]. Acquiring isotopic information of suspended and sinking particles over different seasons helps to pin down when, how and to what extent N fixation may contribute to nitrogen inventory in the deep ocean.

[3] High water temperature (above 20°C), low availability of reactive nitrogen, a stratified water column and presence of bioavailable iron are preferred environmental factors for nitrogen fixation [Karl *et al.*, 1997]. The geographical setting of the South China Sea (SCS), the second largest marginal sea in the world [Liu *et al.*, 2010], offers favorable environmental features for nitrogen fixation [Chao *et al.*, 1996; Wong *et al.*, 2002]. Among the relatively small number of measurements on the rates of nitrogen fixation in the world ocean, the rates observed in the SCS were among the highest values reported [Capone *et al.*, 1997, and references therein], and comparably high rates were also observed in the adjacent areas, like the Kuroshio Current (KC) and East China Sea [Chen *et al.*, 2008; Shiozaki *et al.*, 2010].

¹Research Center for Environmental Changes, Academia Sinica, Taipei, Taiwan.

²State Key Laboratory of Marine Environmental Science, Xiamen University, Xiamen, China.

³Institute of Hydrological Sciences, National Central University, Jhongli, Taiwan.

⁴Institute of Marine Environmental Chemistry and Ecology, National Taiwan Ocean University, Keelung, Taiwan.

⁵Institute of Marine Geology and Chemistry, National Sun Yat-Sen University, Kaohsiung, Taiwan.

⁶Lamont-Doherty Earth Observatory, Columbia University, Palisades, New York, USA.

Corresponding author: S.-J. Kao, Research Center for Environmental Changes, Academia Sinica, Section 2, 128 Academia Rd., Taipei 115, Taiwan. (sjkao@gate.sinica.edu.tw)

©2012. American Geophysical Union. All Rights Reserved.

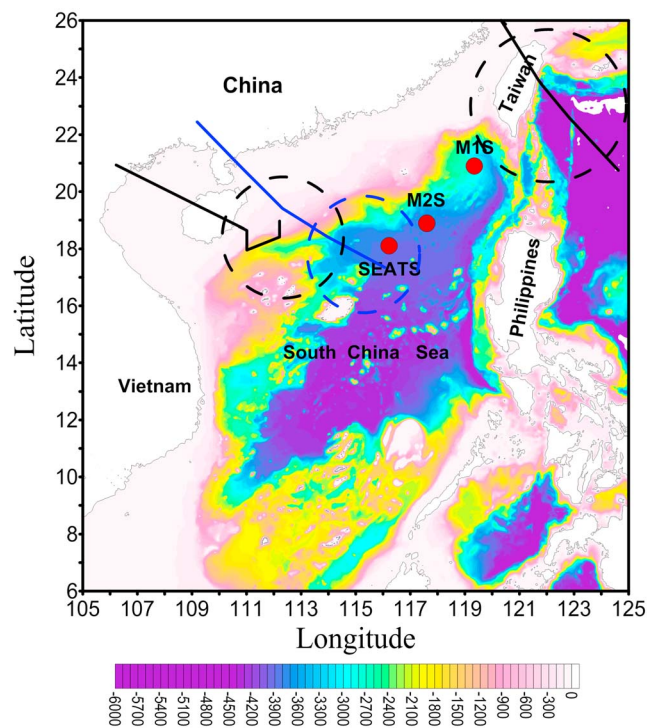


Figure 1. Location of sampling sites in the northern South China Sea. The solid lines and the dashed circles denote the pathways and influence areas of the typhoons swept over our study area, respectively (black for the Typhoons Washi and Haitang in 2005, blue for the Typhoon Jelawat in 2006).

[4] The surface circulation and the biogeochemistry in the SCS are subject to the forcing of the East Asian monsoons [Liu *et al.*, 2002]. Interannual variations in the SCS circulation are mostly associated with modulation of the monsoon strength by El Niño–Southern Oscillation events [Chao *et al.*, 1996]. Total concentrations of nitrate plus nitrite in the mixed layer rise above the detection limit to up to $\sim 0.7 \mu\text{mol kg}^{-1}$ in the winter, but drop below the detection limit in the rest of the year [Chou *et al.*, 2006; Wong *et al.*, 2007a]. However, drawdown of CO_2 continues as indicated by the decline of dissolved inorganic carbon (DIC) for a period of time with nondetectable nitrate in the surface water. The continuing net carbon uptake is likely sustained by the supply of new nitrogen derived from nitrogen fixation [Chou *et al.*, 2006]. Also, a distinctly high-nitrate anomaly (N^* , up to $\sim 2 \mu\text{M}$) with a corresponding low $\delta^{15}\text{NO}_3^-$ in the upper nitracline at the SouthEast Asian Time-series Study (SEATS) station (115.61°E , 18.01°N) (Figure 1) has been interpreted as a result of remineralization of biomass resulting from nitrogen fixation [Wong *et al.*, 2002]. However, whether this is a cumulative signal of regional N fixation or fresh input from diazotrophs in the SCS remains unclear. Nevertheless, it is widely accepted that the ecosystem in the SCS is limited by bioavailable nitrogen. In winter, nutrients are mainly supplied diapycnally from the subsurface waters, where the nutrient reserves have N/P ratio lower than the Redfield ratio [Wu *et al.*, 2003], as cooling and wind stress are intensified. By contrast, when mixing is weak, nitrogen fixation could play an important role in supplying bioavailable nitrogen, which will be taken

up by nondiazotrophic phytoplankton in time [Mulholland, 2007].

[5] Apart from monsoons, the episodic tropical cyclone (typhoon) may also pump up nutrients into the mixed layer. These events can contribute as much as 20–30% of annual new production in the SCS, given an average of 14 typhoons traversing the SCS each year [Lin *et al.*, 2003]. Moreover, increasing quantities of anthropogenic-sourced atmospheric nitrogen deposition to the open ocean may serve as a remarkable external nitrogen supply in oligotrophic marginal seas, such as the SCS [Duce *et al.*, 2008, and references therein]. Strong seasonality in stratification versus various nutrient supply pathways in different seasons provides us an opportunity to explore formation, transportation and transformation of particulate nitrogen in this dynamic marine system.

[6] From the perspective of paleoceanographic research, the nitrogen isotopic composition of sedimentary organic matter has been widely used to infer past changes in biogeochemical dynamics at a given core site [Altabet, 1996]. However, there have been few, if any, studies, in which the seasonal variations of nitrogen isotopic composition of suspended particles in the upper water column were examined; let alone a detailed mechanistic investigation of the processes responsible for the nitrogen isotopic composition of organic matter during its transportation to depths. The SEATS project [Tseng *et al.*, 2005; Wong *et al.*, 2007b] allowed us to conduct seasonal sampling of the suspended particles; at the same time, the sediment traps deployed in the subsurface layer at $\sim 500 \text{ m}$ in the northern SCS have provided samples of sinking particles for comparison. In this study, we compare seasonal changes in isotopic composition ($\delta^{15}\text{N}_{\text{PN}}$) of suspended and sinking particles with related parameters, such as the mixed-layer depth, nitrate concentration and nitrate anomaly (N^*). This study advances our understanding of the seasonal nitrogen supply to the euphotic zone, and dynamical isotopic compositions between suspended and export particles in the upper 400 m, which benefits future modeling work and paleostudies in the South China Sea.

2. Materials and Method

2.1. Sample Collection

[7] Water samples were collected for suspended particulate matter on nine cruises between May 2004 and January 2007 at the SEATS Station (Figure 1 and Table 1) using a

Table 1. Sampling Cruises for the Collection of Suspended Particulate Nitrogen

Cruise	Date	Depth Range	Number of Samples
OR1-717	6 May 2004	0–200 m	9
OR1-726	6 Aug 2004	0–200 m	11
OR1-743	22 Jan 2005	0–200 m	16
FR1-SC33	30 Mar 2005	0–200 m	20
FR1-SC34	30 Jul 2005	0–200 m	17
OR1-780	25 Dec 2005	0–200 m	10
FR1-SC37	5 Jul 2006	0–200 m	10
OR1-812	20–22 Oct 2006	0–200 m	19
OR1-821	16 Jan 2007	0–200 m	20

CTD-rosette sampling system with 20 L GoFlo bottles for sampling on board R/V Ocean Researcher I. On the FR1 cruises, 10 L GoFlo bottles were used (Table 1). Nine to 20 samples were collected on 1–3 hydrocasts depending on the individual cruise schedule. Salinity and temperature were recorded during each cast with a SeaBird model SBE9/11 conductivity-temperature-depth (CTD) recorder. The mixed-layer depth (MLD) was defined as the layer of water holding a density gradient less than 0.125 kg m^{-4} [Suga *et al.*, 2004].

[8] About 10 L of seawater was filtered through a pre-combusted (500°C for 4 h) Whatman quartz filter (25 mm diameter, $1.0 \mu\text{m}$ pore size) to collect suspended particulate matter (SPM). After the filtration, the filters were folded and wrapped in aluminum foil and stored at -20°C until analysis.

[9] We used time series sediment traps (Technicap PPS 3/3, France) to collect sinking particles. Two traps were deployed near the SEATS Station (Figure 1). Trap M1S was deployed at $\sim 374 \text{ m}$ (119.28°E , 21.31°N) during September 2001 through March 2002. Trap M2S was situated at $\sim 447 \text{ m}$ (117.30°E , 19.00°N) during December 2001 through May 2002. The sampling interval was 15 days. Before deployment, all collecting cups were filled with a buffered (5% or 1.7 M) formalin solution ($7.5 < \text{pH} < 8.0$) for sample preservation. A detailed description of pretreatment for trap samples has been given by *K. K. Liu et al.* [2007]. Briefly, samples were stored below 4°C before being transported to the laboratory. Large particles including zooplankton and other swimmers were screened out by a 1 mm Teflon sieve and by hand picking. The sinking particles were then filtered onto a preweighted 47 mm Millipore filter ($0.45 \mu\text{m}$ pore size), which was subsequently washed with deionized water to remove salts. The desalted sample was dried at 40°C for 48 h and then the sample was scraped off from the filter, ground to powder and stored in an auto-desiccator until it was analyzed.

2.2. Isotopic and Chemical Analyses

[10] Filters with suspended particles were freeze dried. Filters were acidified with 1 mL of 1 N HCl solution to remove carbonate after picking off visible zooplankton. This acid pretreatment has been applied in previous studies [e.g., Casciotti *et al.*, 2008; Loick *et al.*, 2007]. All filters were dried at 60°C in an oven for 48 h. The sediment trap samples were treated with 2 mL of 1 N HCl solution to remove carbonate and then dried at 60°C for 48 h. The decarbonated samples were analyzed for total nitrogen contents and their isotopic compositions in a continuous flow elemental analyzer (Carlo-Erba EA 2100) and isotope ratio mass spectrometer (Thermo Finnigan Delta^{plus} Advantage) system. Through this analysis, we obtain both particulate organic carbon (POC) and PN contents with precision $<1\%$ for the standard measurement.

[11] The nitrogen isotopic ratio ($^{15}\text{N}/^{14}\text{N}$) was calibrated to working standards and is presented by δ notation:

$$\delta^{15}\text{N} = \left\{ \left(\frac{^{15}\text{N}/^{14}\text{N}}{\text{sample}} \right) / \left(\frac{^{15}\text{N}/^{14}\text{N}}{\text{standard}} \right) - 1 \right\} \times 1000(\text{‰}) \quad (1)$$

[12] Data were converted to the reference atmospheric N_2 with a $\delta^{15}\text{N} = 0 \text{ ‰}$. The long-term reproducibility of nitrogen isotope determination for the international (USGS 40, L-glutamic acid: $-4.5 \pm 0.1 \text{ ‰}$), working (Merck Acetanilide: $-1.5 \pm 0.2 \text{ ‰}$) standards and field samples is better than 0.2 ‰ .

[13] Dissolved nitrate and nitrite (N + N) concentrations were measured by the standard pink azo dye method with a flow injection analyzer, and phosphate was determined manually by the standard molybdenum blue method [Wong *et al.*, 2007a, and references therein]. The precisions of the determinations of (N + N) and phosphate were ± 0.3 and $\pm 0.01 \mu\text{M}$, respectively. As for the N anomaly, N^* , we followed the definition by *Deutsch et al.* [2001] as $\text{N}^* = [\text{NO}_3^-] - 16 \times [\text{PO}_4^{3-}] + 2.9$ (unit in μM).

3. Results

3.1. Isotopic Compositions of Suspended Particulate Nitrogen

[14] A T-S (temperature-salinity) diagram (Figure 2) for observations on all the sampling occasions indicates that the water masses in the upper water column at the SEATS Station were influenced by the intruding Kuroshio Water (KW) as reported previously [Wong *et al.*, 2007b]. The T-S field (box in Figure 2) of KW was located at a water depth of $\sim 250 \text{ m}$. The consistent T-S characteristics suggest the water column below 250 m was uniform with no seasonality.

[15] Figure 3 presents the vertical profiles of PN concentration and $\delta^{15}\text{N}_{\text{PN}}$ value, as well as N + N concentrations (shown as NO_3^-), from the surface down to a depth of 200 m. The PN concentration profiles often showed a subsurface maximum in the upper 50 m, where the N + N concentration was at or below the detection limit in all but one case in May 2004, during which the maximal PN concentration ranged from 0.22 to $0.36 \mu\text{M}$ with an exceptionally high value of $0.6 \mu\text{M}$. Below the subsurface maximum, all profiles showed a clear decreasing trend in PN concentration to 200 m (ranged from 0.06 to $0.14 \mu\text{M}$). In the mixed layer, the nitrate and phosphate (not shown) concentrations were mostly below the detection limit, but increased to near 15 and $3 \mu\text{M}$, respectively, at 200 m in all cases (Figure 3). The $\delta^{15}\text{N}_{\text{PN}}$ values varied from 0 to 8.0 ‰ in the euphotic zone. Our observed $\delta^{15}\text{N}_{\text{PN}}$ values are consistent with those reported for PN in the western SCS [Loick *et al.*, 2007]. All except two $\delta^{15}\text{N}_{\text{PN}}$ profiles (August 2004 and October 2006) exhibited an increasing trend with depth below the PN maximum.

[16] To reveal the monsoon forcing, Figure 4 shows the time series data of the observed MLD and the daily wind speed in the vicinity of the SEATS Station (from the Reanalysis Project data of NCEP at <http://www.esrl.noaa.gov/psd/data/reanalysis/reanalysis.shtml>). The cyclic curve is derived by using all available MLD data collected at SEATS (see Figure 5a) including period of 1999–2003 reported by *Tseng et al.* [2005]. Similarly, we presented the depth integrated PN (IPN), which represents the PN inventory, and the concentration-weighted average $\delta^{15}\text{N}_{\text{PN}}$ values with empirically fitted cyclic functions in Figure 4. We estimated separately for the water column at 0–100 m (hereafter top 100 m) and 100–200 m (lower 100 m). The

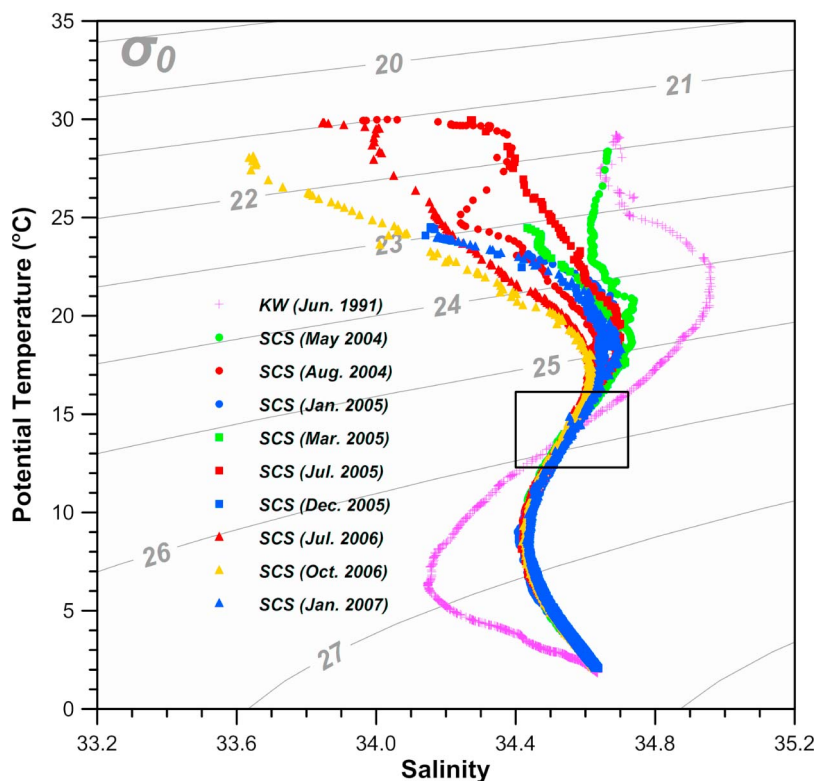


Figure 2. Potential temperature-salinity (T-S) diagram for all sampling occasions at the SEATS station. The purple crosses indicate the Kuroshio Water (KW). The T-S points in the black box locate at 200–300 m interval (see text).

depth of 100 m, the bottom of the euphotic zone and the lower bound of seasonal mixed layer, was set for integration since recycled production will be mainly occurring in the euphotic zone.

[17] The variation of the MLD (Figure 4b) mimics the seasonal pattern of the wind (Figure 4a): deepening of the mixed layer reaching 100 m occurred in winter while the strong northeast monsoon prevailed, subsequent shoaling in spring when the wind subsided, and slight deepening in summer when the southwest monsoon picked up. The high frequency variability of the wind speed was missing in the sparsely spaced time series observations, partially attributed to the damping effect of the water. The more pronounced deepening of the MLD corresponded to the winter monsoons, which are in general stronger and more persistent than the summer monsoons. Another episodic event in summer is typhoons (Figure 1), which can cause strong vertical mixing in the SCS to 200 m temporarily [Lin *et al.*, 2003]. Thus such a cyclic MLD curve in fact represents a mean seasonal pattern of nonevent periods since all cruises were conducted under nontyphoon conditions.

[18] The IPN of the top 100 m shows a cyclic behavior (Figures 4c and 5b) varying between 14 and 42 mmol N m⁻² with higher values in spring and autumn (Table 2) corresponding to the shallowest MLD. Compared to the top 100 m, the IPN in the lower 100 m showed considerably lower values and narrower variability (7–14 mmol N m⁻²). Nevertheless, the seasonal variation in the subsurface layer broadly agrees with that in the top 100 m.

[19] The concentration-weighted average $\delta^{15}\text{N}_{\text{PN}}$ in the top 100 m (Figures 4d and 5c and Table 2) varied between 2.0 and 5.3 ‰ with a mean value of 4.2 ± 1.0 ‰ of all cruises. The low values appeared mainly in spring and fall when the MLD was at its minimum. The $\delta^{15}\text{N}_{\text{PN}}$ values in the lower 100 m showed a similar pattern of seasonal variation but shifted consistently to a range of higher values (4.0–7.8 ‰) (Table 2). Such consistent increase in $\delta^{15}\text{N}_{\text{PN}}$ values in the subsurface layer is similar observations in the Pacific [e.g., Saino and Hattori, 1987; Casciotti *et al.*, 2008] and the Atlantic [e.g., Altabet, 1988] oceans. To ensure the integrated $\delta^{15}\text{N}_{\text{PN}}$ in the top 100 m is representative, we also integrated $\delta^{15}\text{N}_{\text{PN}}$ values for water column above the nitracline, which is shown in Figure 5c for comparison. No significant difference can be observed in between the two depth integrations. Hereafter, we still use 100 m to separate the upper and lower water columns.

[20] POC concentrations were linearly correlated with PN concentrations at the SEATS Station with a regression slope of 5.88 ($R^2 = 0.92$, not shown), which is close to the Redfield C/N ratio of 6.63. According to the observed C/N ratios and reported $\delta^{13}\text{C}_{\text{POC}}$ values [K. K. Liu *et al.*, 2007], we may conclude that the suspended particles in upper 200 m at the SEATS Station were mainly of marine origin with negligible contribution from terrestrial sources.

3.2. Isotopic Compositions of Sinking Particulate Nitrogen

[21] Nitrogen isotopic compositions of sinking particles and their PN fluxes collected by sediment traps are shown in

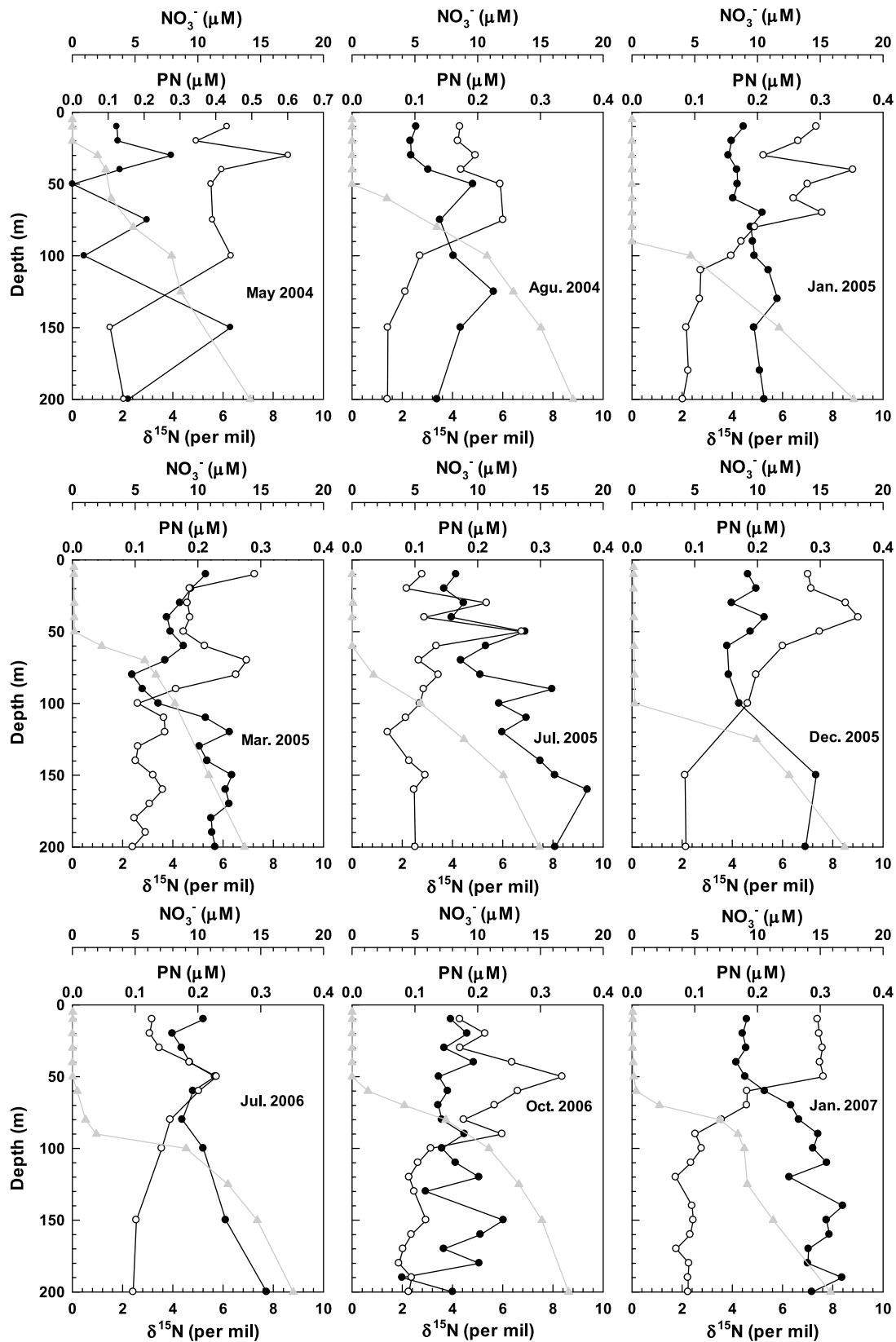


Figure 3. Vertical profiles of suspended PN concentration (open circles) and its $\delta^{15}\text{N}$ value (solid circles) in the upper 200 m observed at the SEATS station on the nine cruises of this study. The nitrate concentration is also shown (gray triangles).

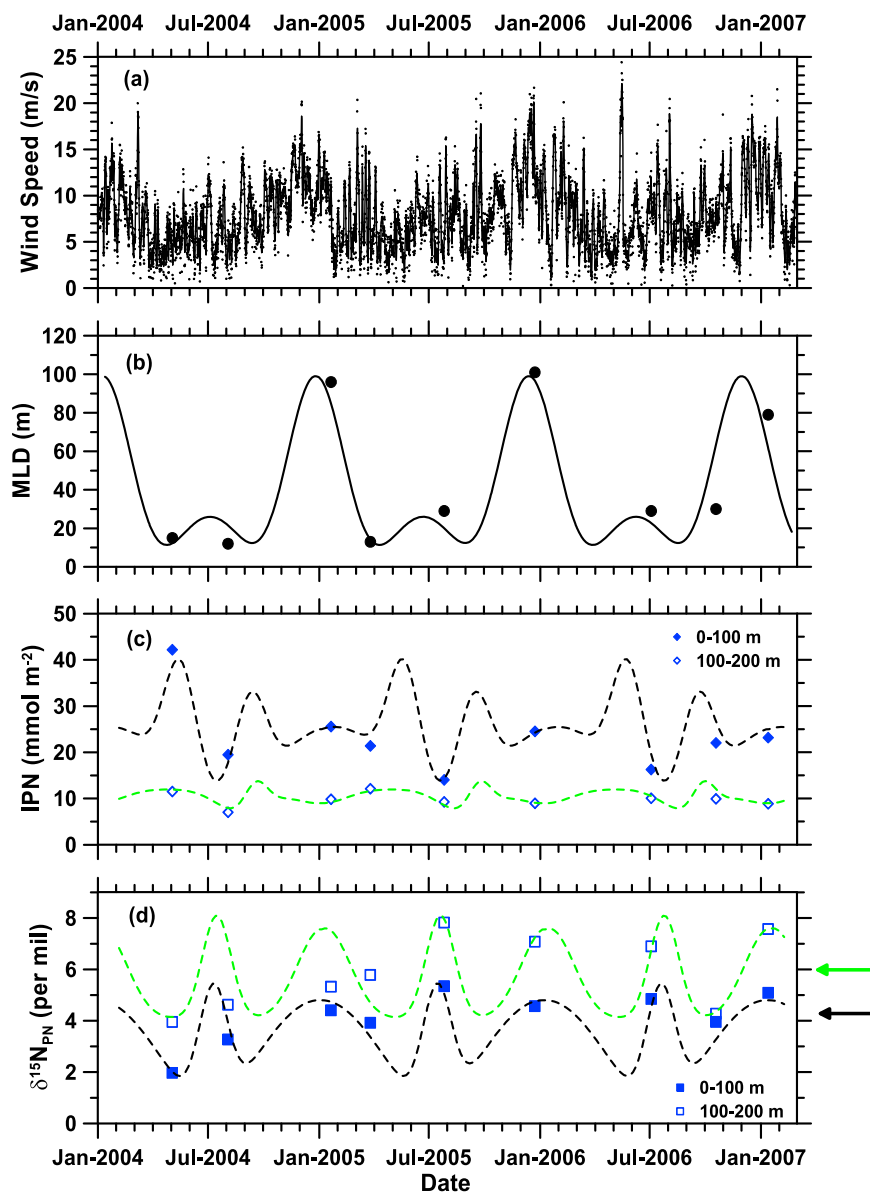


Figure 4. Time series of (a) the wind speed, (b) the mixed-layer depth, and (c) the suspended PN inventory integrated (IPN), and (d) the concentration-weighted average $\delta^{15}\text{N}$ values of the SPM. The dashed curves are empirical fits of cyclic functions over an annual cycle to the observations as shown in Figure 5 (see text). The black and green arrows indicate the average $\delta^{15}\text{N}$ values of the SPM in top 100 m and in lower 100 m over 3 years, respectively.

Figure 6a. For comparison, also plotted are the C/N ratios determined for the trap samples (Figure 6b).

[22] The PN fluxes measured at 374 m of the M1S site varied between 2.7 and 16.7 $\text{mg m}^{-2} \text{d}^{-1}$, and those observed at 447 m of the M2S site are slightly higher ranging from 7 to 66 $\text{mg m}^{-2} \text{d}^{-1}$ with an unusually high peak in April 2002 deserving further discussion (see below). The fluxes were relatively high in February and March at both sites.

[23] The $\delta^{15}\text{N}$ values of sinking PN (Figure 6a) collected at 374 m of the M1S site ranged from 3.3 to 6.6 ‰ with a flux-weighted average of 5.2 ± 1.1 ‰, while those at 447 m of the M2S site ranged from 4.0 to 7.6 ‰ with a flux-weighted average value of 5.5 ± 1.3 ‰. The overall

distribution of the $\delta^{15}\text{N}$ values of sinking PN showed a broad peak occurring from mid-January to mid-March. The peak roughly corresponded to the relatively higher values of the PN fluxes except for the aforementioned unusual peak (Figure 6a).

[24] Three exceptionally high C/N ratios of >14.2 observed at the M2S site indicating a relatively stronger terrigenous signal [K. K. Liu *et al.*, 2007]. Following K. K. Liu *et al.* [2007], the $\delta^{15}\text{N}$ values of three samples are corrected by a simple mixing model based on the C/N ratio (6.63 for marine and 22 for terrestrial) and the $\delta^{15}\text{N}$ value ($\delta^{15}\text{N}$ of 5.0‰ for the terrestrial, which is the mean value of the surface sediment in the northern shelf of the SCS reported by Kienast [2000]). The corrected $\delta^{15}\text{N}$ values

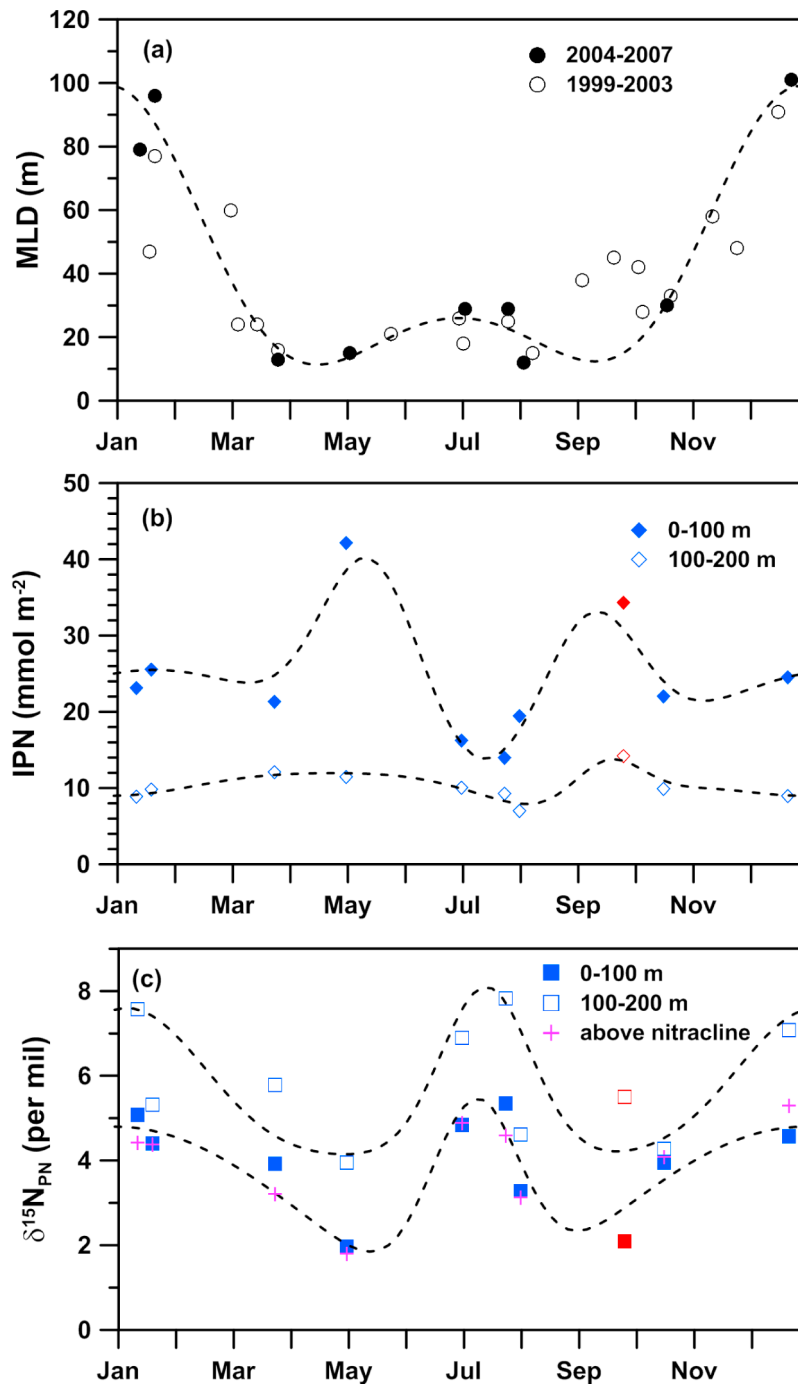


Figure 5. Composite seasonal variations of (a) the mixed-layer depth, (b) the integrated PN in the top 100 m versus lower 100 m, and (c) the concentration-weighted average $\delta^{15}\text{N}_{\text{PN}}$ of the top 100 m and those above nitracline (+) and that of 100–200 m. The solid and open circles in Figure 5a indicate our observed data and the data reported by *Tseng et al.* [2005], respectively. The dashed curves are empirical fits of cyclic functions to the observed data over an annual cycle. The curve fitting also includes previously published data obtained on 27 September 1981 at 117.00°E, 18.09°N in the South China Sea near the SEATS Station [*Saino and Hattori*, 1987].

(black solid circles in Figure 6a) were shifted by 0.6 to 2 ‰. The flux-weighted average of the $\delta^{15}\text{N}$ value in sinking PN collected at 447 m of the M2S site was shifted from 5.5 to 5.6 ‰. The correction shows insignificant influence on the overall pattern of isotopic variation of

sinking PN. Nevertheless, the corrected values should better represent $\delta^{15}\text{N}$ of marine sourced organics, therefore, were used for further discussion of particle dynamics and bioavailable nitrogen sources in the upper water column.

Table 2. The Concentration-Weighted Average $\delta^{15}\text{N}_{\text{PN}}$ and Integrated PN (IPN) of the Top 100 m and the Lower 100 m Observed From May 2004 to January 2007^a

Season	Date	Mean $\delta^{15}\text{N}_{\text{PN}}$ (0–100 m)	Mean $\delta^{15}\text{N}_{\text{PN}}$ (100–200 m)	IPN (0–100 m) (mmol N m ⁻²)	IPN (100–200 m) (mmol N m ⁻²)
Spring	May 2004	2.0‰	4.0‰	42.2	11.5
	Mar 2005	3.9‰	5.8‰	21.4	12.1
Summer	Aug 2004	3.3‰	4.6‰	19.5	7.0
	Jul 2005	5.3‰	7.8‰	14.0	9.3
	Jul 2006	4.9‰	6.9‰	16.3	10.1
Autumn	Oct 2006	4.0‰	4.3‰	22.0	9.9
	Sep 1981	2.1‰	5.5‰	34.3	14.2
Winter	Jan 2005	4.4‰	5.3‰	25.6	9.8
	Dec 2005	4.6‰	7.1‰	24.5	9.0
	Jan 2007	5.1‰	7.6‰	23.2	8.9

^aValues obtained from Station 5 in September 1981 [Saino and Hattori, 1987], which was located near the SEATS Station (see text), were compiled.

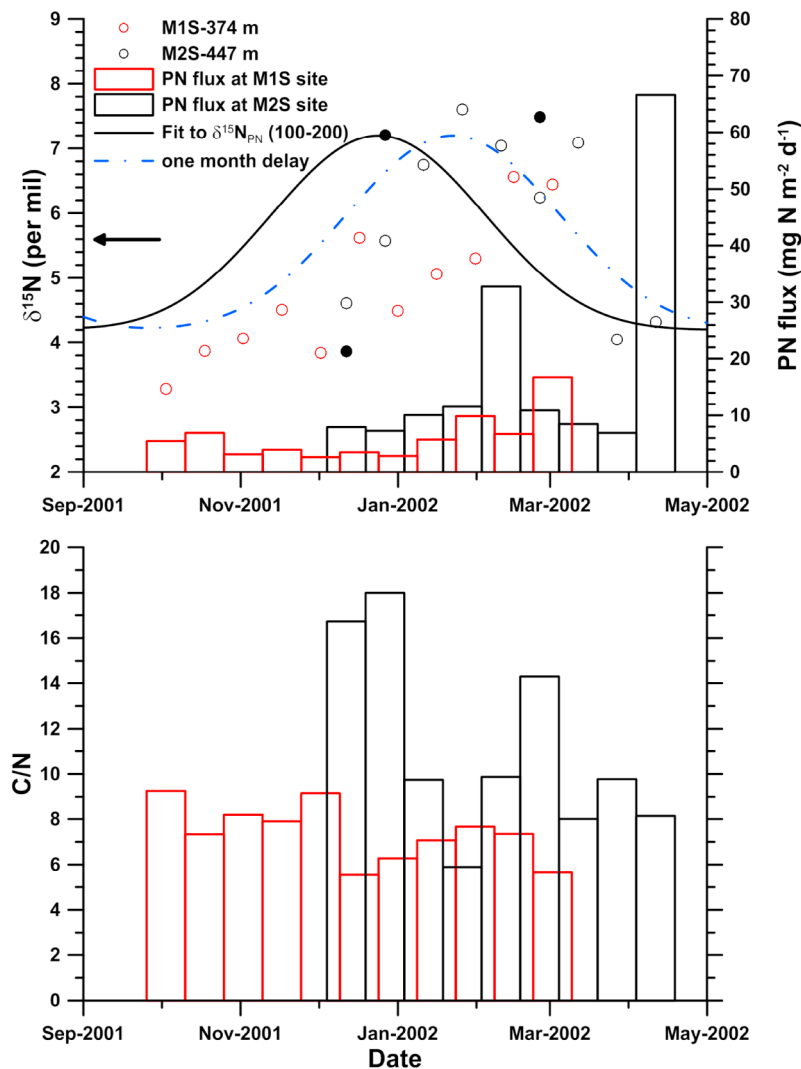


Figure 6. Time series of the (top) $\delta^{15}\text{N}$ value (open circles) and PN flux and (bottom) C/N ratio of sinking particles collected by sediment trap at 374 m of the M1S site (red) from 22 September 2001 to 20 March 2002 and at 447 m of the M2S site (black) from 16 December 2001 to 14 May 2002. The solid black circles represent the $\delta^{15}\text{N}$ values corrected by removing the terrestrial influences (see text) from the M2S site. The black arrow indicates the flux-weighted average $\delta^{15}\text{N}$ value of the sinking particles from the two sites. (Note that the corrected values are included in the averaging.) The solid curve is the fit to the seasonal variation of concentration-weighted average $\delta^{15}\text{N}_{\text{PN}}$ values from the lower 100 m at the SEATS site (see Figure 5c). The blue curve denotes the empirical fit (solid line) being shifted 1 month forward.

[25] It is interesting to note that the isotopic composition of the sinking PN appears to follow the seasonal trend of the suspended PN in the lower 100 m with a 1 month lag (Figure 6a). Conceivably the suspended PN in the subsurface layer represents the particulate materials that sink out of the surface layer and disintegrate to become the suspended particles, while the lag time could be attributed to reaggregation in the subsurface layer and subsequent downward transport to the sediment traps several hundred meters below. It is also noteworthy that most of the data points of the sinking particles fall below the curve of the suspended particles, suggesting that the $\delta^{15}\text{N}_{\text{PN}}$ in the lower 100 m represent the upper limit of the isotopic composition of the sinking PN.

4. Discussion

4.1. Controls of Vertical Distribution of Particulate Nitrogen Isotope

[26] The SPM in the upper open ocean is mainly derived from phytoplankton. The nitrogen isotopic composition in SPM is controlled by many factors, among which the origin of the nitrogen used during its synthesis is perhaps the most important. Other factors include the isotopic fractionation during its formation and the subsequent degradation and alteration processes.

[27] At the SEATS Station, the practically absent nitrate in the surface layer all year round implies its rapid and essentially complete consumption by phytoplankton. Since the near complete consumption of nitrate causes little or no isotopic fractionation, the $\delta^{15}\text{N}$ of the freshly produced SPM should reflect the isotopic compositions of its nitrogen sources [Altabet, 1988; Gaye et al., 2009].

[28] The $\delta^{15}\text{N}_{\text{NO}_3}$ of the subsurface water, which is the main nutrient reserve for the euphotic zone, plays a critical role in controlling the $\delta^{15}\text{N}$ of suspended PN in the overlying surface layer. In the case of the northern SCS, the supply of ^{15}N -replete nitrate from the subsurface nutrient reserve should be the major N source driven by various nutrient pumping processes, such as basin-wide active upwelling (90 m yr^{-1} [Qu et al., 2006]), monsoon-driven localized upwelling and the prevailing northeasterly monsoon in winter and episodic tropical cyclones in summer [Liu et al., 2002; Lin et al., 2003; Liu et al., 2010].

[29] The mean $\delta^{15}\text{N}_{\text{PN}}$ value ($4.2 \pm 1.0 \text{ ‰}$) in top 100 m is higher than $\delta^{15}\text{N}_{\text{PN}}$ reported for other low-latitude oligotrophic oceans (e.g., -0.9 to 0.8 ‰ in the Sargasso Sea [Altabet, 1988], and 0.5 – 1.1 ‰ at ALOHA Station [Casciotti et al., 2008]). Aside from the higher $\delta^{15}\text{N}_{\text{PN}}$ values, $\delta^{15}\text{N}_{\text{NO}_3}$ at 200–300 m at SEATS is also higher than the mean $\delta^{15}\text{N}_{\text{NO}_3}$ value ($2.65 \pm 0.32 \text{ ‰}$) near Bermuda [Knapp et al., 2005] or the reported 1.9 to 6.1‰ near Hawaii [Casciotti et al., 2008] at depth of 200–300 m. Unfortunately, we have only one reported $\delta^{15}\text{NO}_3$ value of 6.2‰ below the permanent thermocline near SEATS Station [Wong et al., 2002]. Nevertheless, $\delta^{15}\text{N}_{\text{PN}}$ values in top 100 m are consistently lower than $\delta^{15}\text{N}_{\text{NO}_3}$ in subsurface layer at all three oligotrophic regions.

[30] On the other hand, isotope fraction during mineralization may account for the downward increasing trend in $\delta^{15}\text{N}_{\text{PN}}$ value. The mean of isotopic fractionation factor between top and lower 100 m is 2.2‰, which resembles

estimates from lab experiments [Sigman et al., 2009, and references therein]. Preferential turnover of light nitrogen sourced from sinking particles and dissolved organic nitrogen may result in such a vertical pattern in $\delta^{15}\text{N}_{\text{PN}}$ [Altabet, 1988; Saino and Hattori, 1987; Knapp et al., 2011].

[31] Near Bermuda, particles collected by traps deployed at 100 m had higher $\delta^{15}\text{N}_{\text{PN}}$ values than the suspended PN from 0 to 100 m by 3.5 ‰ on average [Altabet, 1988]. Similarly, the $\delta^{15}\text{N}_{\text{PN}}$ of 150–500 m trapped particles were higher by 1.0–4.4 ‰ near Hawaii [Karl et al., 1997]. In our case, the particles collected by traps deployed at 374 m and 447 m had flux-weighted mean $\delta^{15}\text{N}$ values of 5.2–5.6 ‰, which are higher than those in the top 100 m by 1.6 ‰ on average. Like most oligotrophic oceans, regenerated ammonia may play an important role to support photosynthesis at SEATS [Chen, 2005]. It has long been proposed that the regenerated ammonia via zooplankton grazing is depleted in ^{15}N , which is corroborated by the production of ^{15}N -enriched fecal pellets observed in laboratory experiments [e.g., Checkley and Entzeroth, 1985]. Moreover, recent findings showed that preferential uptake and subsequent transport by specific phytoplankton community [Fawcett et al., 2011] may also induce such a downward increasing pattern.

4.2. Seasonal Variations of the Suspended PN and Its Isotopic Composition

[32] The annual cycle of $\delta^{15}\text{N}_{\text{PN}}$ variations in the two layers somewhat resembled that of the MLD variation (Figure 5) with the lowest $\delta^{15}\text{N}_{\text{PN}}$ values during periods of the shallowest MLD indicating that the seasonal pattern of particulate isotopic composition might be associated with nutrient supply via diapycnal mixing.

[33] The shallowest MLD reflects weak diapycnal mixing, thus, the regenerated production should be the highest to maintain the depression of the $\delta^{15}\text{N}_{\text{PN}}$ values in the top 100 m. This can be supported by the observation that f ratio (integrated new production/integrated primary production) values [Chen, 2005] in spring (0.18–0.36) and autumn (0.15–0.20) were lower than winter (0.47). Interestingly, the two lowest $\delta^{15}\text{N}_{\text{PN}}$ values coincide with the IPN peaks of top 100 m. It is highly unlikely that the regenerated production in spring and autumn would cause IPN peaks. It appears some other mechanisms must be added to support the observed intermonsoonal IPN highs.

[34] In winter the high f ratio is consistent with the physical conditions in the SCS. The f ratio of 0.47 implies that nearly half of the primary production is fueled by nitrate uptake apparently resulting from the strong supply of nitrate by regional upwelling and wind driven mixing [Liu et al., 2002]. The relatively high mean $\delta^{15}\text{N}_{\text{PN}}$ values (4.4–5.1 ‰) in the top 100 m in winter (Figure 5b) apparently originated from the new nitrate pumped up from the subsurface layer, where the $\delta^{15}\text{N}_{\text{NO}_3}$ ranges from 4.8 to 6.2 ‰ [Wong et al., 2002]. When compared with the persistently strong winter monsoons, the summer monsoons are usually weak but could be spiked with occasional tropical cyclones. The relatively wide range of the summer $\delta^{15}\text{N}_{\text{PN}}$ values (3.3–5.3 ‰) suggest different conditions exist for summer. The two high values were likely induced by episodic strong mixing events, such as caused by typhoons. Now the remaining question will be

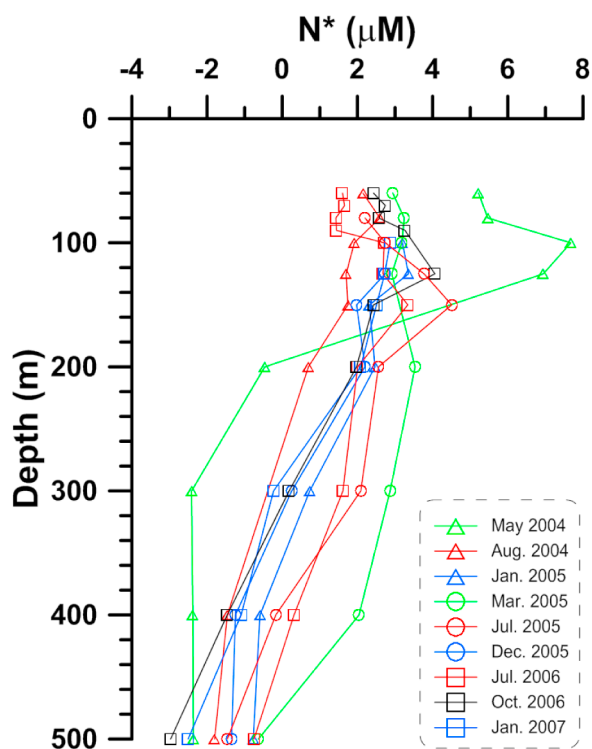


Figure 7. The vertical distributions of N^* in the upper 500 m at SEATS site from May 2004 to January 2007. We omitted the values of N^* when either nitrate or phosphate concentrations were below the detection limit.

the origin of the additional isotopically light nitrogen to increase IPN and decrease the $\delta^{15}N_{PN}$ in spring and autumn.

4.3. Origin of Isotopically Light Nitrogen

[35] Several distinct mechanisms may provide ^{15}N -depleted nitrogen to the surface waters in oligotrophic regions. First, fixation of atmospheric N_2 ($\delta^{15}N = \sim 0$ ‰) by marine diazotrophs is considered a significant source of new nitrogen [e.g., Karl *et al.*, 1997; Montoya *et al.*, 2004; Mahaffey *et al.*, 2005]. Little fractionation occurs during N_2 fixation, resulting in a $\delta^{15}N$ of -2 to 0 ‰ for the newly fixed nitrogen [Carpenter *et al.*, 1997], which could lower the $^{15}N/^{14}N$ ratio of particulate and dissolved species in the upper water column. Second, atmospheric precipitation generally contains inorganic nitrogen with distinctively low $\delta^{15}N$ values [Hastings *et al.*, 2003; Jia and Chen, 2010] and high atmospheric deposition (~ 1000 mg N m^{-2} yr^{-1} or even higher) had been reported for Asian marginal seas [Duce *et al.*, 2008].

[36] Quite a few studies provide geochemical evidence of widespread occurrences of N_2 fixation in the SCS [e.g., Wong *et al.*, 2002; Chou *et al.*, 2006]. Positive N^* , corresponding to lowered $\delta^{15}NO_3^-$, indicates the significant contribution from the remineralization of organics formed by N_2 fixation [Wong *et al.*, 2002]. By means of a box model of nitrogen budget at the SEATS Station, Chou *et al.* [2006] concluded that N_2 fixation by unicellular cyanobacteria as well as by *Trichodesmium* and *Richelia* could provide the additional bioavailable nitrogen required for net community production.

[37] At the SEATS Station over the 3 year observation periods our own records reveal an upward increasing trend in N^* values from <0 at ~ 500 m up to ~ 4 μM at ~ 100 m (Figure 7). It is conceivable that nitrogen fixation plays a role in introducing ^{15}N -depleted nitrogen to the SPM pool at the SEATS Station from May 2004 to January 2007, particularly, the highest N^* had occurred in May 2004 corresponding to the peak IPN and lightest $\delta^{15}N_{PN}$ values. The shallow MLD during the intermonsoon seasons resulted in weakened vertical transport of subsurface nitrate and favored the occurrence of nitrogen fixation. This presents a plausible mechanism to explain the depressed $\delta^{15}N_{PN}$ values in spring and autumn.

[38] Moreover, the proposed onset of nitrogen fixation in spring was in phase with the atmospheric deposition of land-derived dusts and aerosols in the northern SCS, which could have supplied the dust-carried iron to the P-replete (5 – 20 nM) but low available iron (~ 0.2 – 0.3 nM) condition in the surface water [Wu *et al.*, 2003]. The exceptionally high N^* observed in May 2004 (Figure 7) reflects an exceptionally strong diazotroph bloom, which was attributable to a strong atmospheric fallout event in early April of 2004 [Hsu *et al.*, 2008]. On the other hand, the biomass burning prevalent in surrounding landmasses of the SCS in August [Lin *et al.*, 2007] could produce aerosols that may possibly enhance nitrogen fixation in early autumn as the summer monsoon subsides.

[39] We admit that the direct atmospheric bioavailable N input might contribute, yet, it is difficult to validate due to the lack of field observations on fluxes and isotopic compositions of fixed nitrogen in wet and dry depositions in SCS proper. We will discuss the potential of atmospheric N input in section 4.6.

4.4. Fate of Nitrogen Fixation Signals

[40] It is widely accepted that nitrogen fixation by marine organisms, such as *Trichodesmium* [Carpenter *et al.*, 1997], occurs mostly in the upper water column near the surface. However, little is known about the fate of the marine diazotrophs that carry out this process. To assess the effect of nitrogen fixation on the marine nitrogen and carbon cycles, it is crucial to appreciate whether the N fixation signal is mostly exported to the deep water or remineralized in the upper layer.

[41] Two different pathways for the transfer of the N fixation signals were proposed by Mulholland [2007]: the N fixation signals could be transferred to higher trophic levels and transformed into large-size particulates through the food chain, thus, to enhance the sinking flux. Alternatively, the nitrogen fixers and their phytodetritus could remain mostly in the surface layer for decomposition and recycling because nonsymbiotic diazotrophs are usually not regarded as important contributors to the direct export flux of organic matter from the euphotic zone because of their small size or high buoyancy [Capone *et al.*, 1997].

[42] For our investigation, nitrogen isotope signatures are used to trace the passage of the N fixation signals. Aforementioned data from Sta. Five of Saino and Hattori [1987] are also included for discussion. The seasonal variation of the concentration-weighted average $\delta^{15}N_{PN}$ from the lower 100 m mimics that of the top 100 m as shown in Figure 5c implying that the surface isotopic signals have been

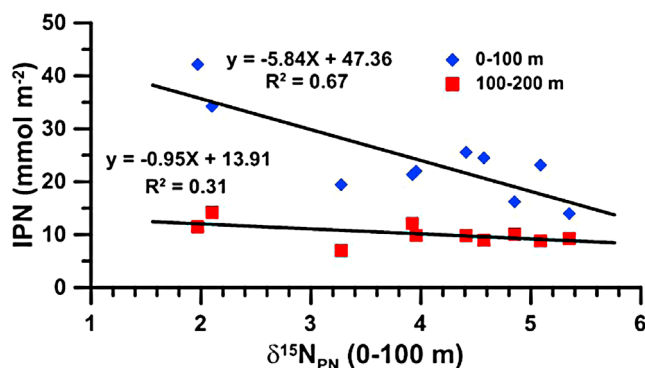


Figure 8. Scatterplot of the integrated PN values in two layers against the concentration-weighted average $\delta^{15}\text{N}_{\text{PN}}$ values in the top 100 m.

transferred to the subsurface layer. Since the IPN inventory in the top 100 m reveals stronger seasonal patterns compared with IPN of 100–200 m, the downward transfer efficiency varies seasonally and the efficiency can be evaluated from the deviation in IPN between the two layers. From Figures 5b and 5c, we notice that the $\delta^{15}\text{N}_{\text{PN}}$ for both layers correlates negatively with IPN in the top 100 m. The highest IPN values correspond to the lowest mean $\delta^{15}\text{N}_{\text{PN}}$ values and may imply high contribution from N_2 fixation. A high IPN probably suggests that the phytodetritus have a longer residence time in the upper water column due to sluggish sinking of the diazotrophs from the surface layer to the subsurface layer.

[43] Diazotrophs in the SCS include all forms of N_2 fixers, filamentous (e.g., *Trichodesmium*), unicellular and symbiotic cyanobacteria [Chen et al., 2008; Chou et al., 2006]. Aside from the symbiotic diazotrophs, the rest do not make it into the sinking particles readily. *Trichodesmium*, likely the most abundant among the three types, are grazed by harpacticoid copepods, which appear tolerant to the often toxic *Trichodesmium* species [O’Neil and Roman, 1994]. An important species of such copepods, *Macrosetella gracilis*, was found in significant amounts in the surface Kuroshio water and the abundance of nauplii was found positively correlated to the *Trichodesmium* chlorophyll concentration (T. Suzuki et al., personal communication, 2011). Since the Kuroshio water intrudes into the SCS periodically [Shaw, 1991], it is very likely that these specialized copepods also exist in the SCS in quantities that are capable of grazing on *Trichodesmium* colonies intensively. Such grazing could quickly convert the newly fixed nitrogen into ammonia either by fast metabolism or by sloppy feeding [O’Neil et al., 1996]. The latter could also produce slow-sinking phytodetritus instead of fast-sinking fecal pellets. The released ammonium could induce quick growth of picoplankton, which is the dominant phytoplankton in the SCS [Chen, 2005; H. B. Liu et al., 2007].

[44] In Figure 8, we plot observed IPN values for both upper and lower layers against the $\delta^{15}\text{N}_{\text{PN}}$ in top 100 m layer. The two negative trends converge at the high-end $\delta^{15}\text{N}_{\text{PN}}$ during which upwelling and the primary productivity are intensified. The phytoplankton composition may be regarded as the background community dotted with modest blooms of diatoms, which occur when nutrient pumping is

more effective [Chen, 2005; Liu and Chai, 2009]. “Normal” food chain activity is in operation such that the primary producers are grazed down and converted into fecal pellets that sink out of the euphotic zone relatively quickly. This explains the reported high primary productivity yet lower particle inventory in euphotic zone in winter. By contrast, at the high end of IPN the upper 100 m holds more ^{14}N -replete SPM due to weaker downward transfer efficiency.

[45] The downward transport of the N fixation signals is further explored by examining the sediment trap data. The $\delta^{15}\text{N}$ values of sinking particles collected by sediment traps at 374–447 m below surface showed significant seasonal contrast over the range from 3.3 to 7.6 ‰, with high values in winter and low values in autumn and spring. As mentioned above, the pattern is somewhat similar to the temporal variation of $\delta^{15}\text{N}_{\text{PN}}$ in the overlying subsurface layer (100–200 m), except that occurrences of the high values lagged behind those in the overlying water column by a month or so (Figure 6). Since the $\delta^{15}\text{N}$ values of sediment trap samples have been adjusted to remove the strong terrigenous signals, the seasonal contrast most likely originated from seasonal variation of N_2 fixation. In other words, the signals of N_2 fixation have been transferred to the sediment trap samples, despite the rather low transfer efficiency in the surface layer. This is supported by the observation that *Trichodesmium* specimens were found in our trap at the depth of 374 m of the M1S site [Chen et al., 2003]. The average flux of *Trichodesmium*, estimated to be 3.6×10^3 trichomes $\text{m}^{-2} \text{d}^{-1}$ during the deployment period, however, was rather small. No trichomes were ever detected in samples from the deeper traps illustrating the limited downward transport of *Trichodesmium*. However, once the diazotrophs are broken down and decomposed, the signal of the regenerated nitrogen should be passed on to other phytoplankton that may undergo the normal food chain sequence so that the signal will be transferred to the deeper water column.

4.5. Assessment of N Fixation Rate Using Isotope Balance

[46] To estimate the relative contributions of nitrate from upwelled deep water and nitrogen fixation in supplying newly combined nitrogen to the new production, we followed a similar approach adopted in other oligotrophic oceans [e.g., Karl et al., 1997; Bourbonnais et al., 2009]. In steady state, the export of sinking PN through 410 m should balance to the sum of the upwelled nitrate and newly fixed nitrogen. Thus, the mass and isotope balances are formulated:

$$\Phi_{\text{EX}} = \Phi_{\text{NO}_3} + \Phi_{\text{N}_2} \quad (2)$$

$$\delta^{15}\text{N}_{\text{EX}} \times \Phi_{\text{EX}} = \delta^{15}\text{NO}_3^- \times \Phi_{\text{NO}_3} + \delta^{15}\text{N}_2 \times \Phi_{\text{N}_2} \quad (3)$$

where Φ_{EX} , Φ_{NO_3} , and Φ_{N_2} represent, respectively, the fluxes of the sinking PN at 410 m, the upwelled nitrate and N_2 fixation, and $\delta^{15}\text{N}_{\text{EX}}$, $\delta^{15}\text{NO}_3^-$ and $\delta^{15}\text{N}_2$ denote the respective nitrogen isotopic compositions.

[47] Instead of calculating for each data point, we use the average values during the deployment periods, which should better reflect the average steady state under which the mass and isotope balances are achieved. We assumed the $\delta^{15}\text{N}$ values of the two influxes of nitrogen ($\delta^{15}\text{NO}_3^-$ and $\delta^{15}\text{N}_2$) to

be 6.1 ‰ and -0.9 ‰, respectively, following those used by *Liu et al.* [1996]. The choice of 6.1 ‰ for the $\delta^{15}\text{N}$ value of supplied nitrate is supported by observations of a ~ 300 m lifting of North Pacific Intermediate Water (NPIW) when the Kuroshio Current intrudes the South China Sea [*You et al.*, 2005]. This isopycnal uplifting induces a shallow thermocline, thus, the $\delta^{15}\text{N}$ values of nitrate observed in the 200–300 m layer in the northern SCS [*Wong et al.*, 2002] are almost identical to those observed at a depth of ~ 600 m in the Kuroshio Current northeast of Taiwan [*Liu et al.*, 1996]. For the sinking PN, the $\delta^{15}\text{N}$ ($\delta^{15}\text{N}_{\text{EX}}$) is assumed to be the flux weighted mean $\delta^{15}\text{N}$ (5.6 ‰, horizontal arrow in Figure 6a) observed from the two traps deployed at 374 and 447 m in the northern SCS. The average sinking flux of PN collected by these two traps ($11.5 \pm 14.6 \text{ mg N m}^{-2} \text{ d}^{-1}$ or $300 \pm 380 \text{ mmol N m}^{-2} \text{ yr}^{-1}$) is taken as the value for Φ_{EX} . An independent approach based on the POC-ballast relationship is used to estimate the value of Φ_{EX} [*Armstrong et al.*, 2002; *Kao et al.*, 2006] to avoid the bias due to incomplete annual coverage of the sediment trap sampling. Surprisingly, this independent approach gives nearly identical value ($\sim 258 \text{ mmol N m}^{-2} \text{ yr}^{-1}$), suggesting the observed mean flux of sinking PN to be representative. By solving equations (2) and (3), the flux of N_2 fixation is estimated to be $21 \pm 26 \text{ mmol N m}^{-2} \text{ yr}^{-1}$.

[48] Compared to previously reported N_2 fixation rate ($5.4 \pm 10.6 \text{ mmol N m}^{-2} \text{ yr}^{-1}$) based on *Trichodesmium* counts in the northern SCS [*Chen*, 2005], our estimated rate was 4 times higher. However, the wide range of individual observations (0.3 to $40 \text{ mmol N m}^{-2} \text{ yr}^{-1}$) indicates the nature of the sporadic and patchy occurrences of *Trichodesmium*. Our estimate is similar in magnitude within the range of actual occurrences in this region.

[49] This estimated N fixation rate represents ~ 5 – 10% of the reported total new nitrogen requirement or 1.5 – 3.3% of the nitrogen needed for primary production [*Chen*, 2005]. This is lower than the estimates of the contribution to the nitrogen needs of primary production (3 – 13%) based on nitrate anomalies observed at the SEATS Station [*Wong et al.*, 2007a]. In *Wong et al.* [2007a], they use N^* as a proxy for the imbalance between N and P supply to the upper ocean of 150 m. This method represents a longer-term cumulative contribution from N fixation to nitrate inventory in the upper 150 m water column. By contrast, our estimate focuses on the fraction of the downward transfer of N fixation signal through the sampling water depth of 410 m. Results for N fixation input from this kind of box model are depth dependent. A higher fractional contribution will be derived if bottom was set at 100 m deep since a portion of N fixation input is recycled.

[50] In addition, *Gaye et al.* [2009] reported that nitrogen fixation could contribute up to 20% of sinking PN through 2000 m in the SCS basin, which was significantly higher than our estimate. It is worth mentioning that the PN flux for the deeper trap is larger than the flux from shallow traps in *Gaye et al.* [2009]. Though terrestrial PN signals had been eliminated, they did not consider the export production induced by riverine nitrate discharge, which equals the amount of N fixation input on a basin scale [*Liu et al.*, 2010]. Basing on our observations, we speculate that N fixation signal can reach such deep water giving a high fractional contribution in on a basin scale. We hypothesize that the

lateral PN (marine PN carried ^{15}N -depleted signal from riverine nitrate/ammonium) transport from shelf to deeper layer in winter may play a role, especially because the shallow shelf occupies $>1/3$ of the basin area receiving huge amount of freshwater input. On the other hand, $\delta^{15}\text{N}$ values for the ~ 400 m sediment trap in our study is higher than the $\delta^{15}\text{N}$ values for materials collected at deep water depths [*Gaye et al.*, 2009; J. Y. T. Yang, unpublished data, 2006]. Many studies have observed a decreasing trend in the $\delta^{15}\text{N}$ of sinking PN with depth [e.g., *Altabet et al.*, 1991]. Some unknown alteration processes (either vertically or laterally or both) might be responsible for this deviation in $\delta^{15}\text{N}$ between deep and shallow sinking particles.

[51] Our estimate is nearly the same as that ($20 \text{ mmol N m}^{-2} \text{ yr}^{-1}$) estimated by *Liu et al.* [2010] for the northern SCS, similar to that ($15 \text{ mmol N m}^{-2} \text{ yr}^{-1}$) reported for the BATS Station [*Orcutt et al.*, 2001] and slightly lower than those (31 – $51 \text{ mmol N m}^{-2} \text{ yr}^{-1}$) reported for the Hawaii Ocean Time series Station [*Karl et al.*, 1997]. Moreover, a similar range for the nitrogen fixation rate (5 – $42 \text{ mmol N m}^{-2} \text{ yr}^{-1}$) was observed in the upwelling region off Vietnam in the western SCS [*Voss et al.*, 2006]. It is reasonable to assume a similar range of N fixation rates occurs in the entire SCS basin, resulting in a calculated nitrogen fixation flux of $0.56 \text{ Tg N yr}^{-1}$.

4.6. Uncertainties

[52] Growing evidence indicates that islands and marginal seas adjacent to China receive significant atmospheric N deposition ($\sim 1000 \text{ mg N m}^{-2} \text{ yr}^{-1}$ or even higher) sourced from inland China emission [*Duce et al.*, 2008; *Zhang et al.*, 2011]. Such a large atmospheric deposition, in fact, is $\sim 3\text{x}$ our estimate of new nitrogen from N fixation and of the same magnitude as the nitrate supply from upwelling. The reported annual mean values of $\delta^{15}\text{N}$ for NO_3^- and NH_4^+ from coastal area of South China, 300 km north of the SEATS Station, were as low as -0.7 ‰ and -7.3 ‰, respectively [*Jia and Chen*, 2010]. If atmospheric ^{15}N -depleted N deposition sourced from inland China can really reach SCS proper, the isotopically light nitrogen should be brought by the winter northeasterly monsoon wind to lower the $\delta^{15}\text{N}_{\text{PN}}$ values significantly at SEATS. However, the $\delta^{15}\text{N}_{\text{PN}}$ values in the winter monsoon season approach the $\delta^{15}\text{N}$ value of upwelled nitrate. Alternatively, if N deposition from the atmosphere is high enough and follows the seasonal precipitation pattern [*Liu et al.*, 2010] of monthly rainfall from May to September, then, the ^{15}N -depleted atmospheric N deposition indeed broadly explains (except cyclone disturbance) the seasonally low $\delta^{15}\text{N}_{\text{PN}}$.

[53] However, the atmospheric deposition of isotopically light bioavailable nitrogen does not explain the observed negative correlation between downward transfer efficiency and $\delta^{15}\text{N}_{\text{PN}}$ in the surface layer, which is presumably caused by diazotrophs and associated ecosystem responses. Meanwhile, a higher abundance of diazotrophs was observed from spring to autumn, which indicates that the surface ocean is N limited. Based on the mass balance of the N budget, *Liu et al.* [2010] reported a dry-wet deposition of N to be $\sim 100 \text{ mg N m}^{-2} \text{ yr}^{-1}$, which is much smaller than model predictions and would account for around one third of our estimated N fixation flux. Further observations on the

seasonal pattern of atmospheric deposition in the SCS at the basin scale are urgently needed.

[54] On the other hand, our model calculation is prone to uncertainties, which are directly related to the reliability of the values used in the calculation. One of the most sensitive variables is the mean $\delta^{15}\text{N}$ value of the sinking particles as emphasized by Knapp *et al.* [2005]. In our case, the sediment trap samples covered 7 months of a year. Better temporal coverage should improve the estimation revealing seasonal variations in N fixation. However, the missing months are from May to September, which is the period of relatively low productivity, and, therefore, may not cause too big a bias as far as the flux-weighted mean value is concerned.

[55] As in most models, we neglect the effect of DON pool, which represents the largest fixed N pools in the oligotrophic surface layer [Knapp *et al.*, 2005]. A significant flux of low $\delta^{15}\text{N}$ -DON derived from N fixation could export out of surface waters [Mulholland *et al.*, 2006], although, many studies argued that a large fraction of DON is recalcitrant [Knapp *et al.*, 2005] and not responsive to the sporadic events of N fixation [Knapp *et al.*, 2011]. On the other hand, we prescribed a steady state for this model which might not be realistic; accumulation of low $\delta^{15}\text{N}$ -DON in surface might cause uncertainties. Apparently, DON concentration and its isotopic composition need to be well studied in order to construct a complete mass balance of fixed N pools in the SCS. Last, the contribution if any from lateral transport of SPM with unknown isotopic composition to sediment trap at ~ 410 m might also cause uncertainties.

5. Conclusions

[56] We first present nitrogen isotopic data of SPM at SEATS Station in the SCS. The concentration-weighted average $\delta^{15}\text{N}$ values of the SPM (mean $\delta^{15}\text{N}_{\text{PN}}$) in the upper 100 m is 4.2 ± 1.0 ‰, which are higher than those observed in other low-latitude oligotrophic oceans, ascribed probably to a stronger supply of ^{15}N -replete nitrate sourced from the deeper waters and driven by various nutrient pumping processes. The mean $\delta^{15}\text{N}_{\text{PN}}$ values in the upper 100 m show significant seasonal patterns strongly correlated to mixed-layer depth. Strong wind during the winter monsoon deepened the mixed layer and brought up more ^{15}N -replete NO_3 into the euphotic zone from the thermocline, whereas lower $\delta^{15}\text{N}_{\text{PN}}$ values correspond to a shallow MLD in the intermonsoon seasons (spring and autumn). A persistent downward increasing in $\delta^{15}\text{N}_{\text{PN}}$ was observed throughout the observation period implying that some biologically mediated preferential downward transfer of isotopically heavy nitrogen, preferential ammonification of ^{14}N in the top 100 m and/or an addition of ^{15}N -depleted N from the atmosphere are required to facilitate such vertical $\delta^{15}\text{N}_{\text{PN}}$ gradient. A good correlation between the mean $\delta^{15}\text{N}_{\text{PN}}$ below 100 m and that in the upper 100 m was found implying that the nitrogen isotope signals in the euphotic zone have been transferred to the subsurface layer. The smallest gradient in IPN (decreasing downward) and $\delta^{15}\text{N}_{\text{PN}}$ (increasing downward), which implies a strong transfer efficiency, appeared in winter time with abundant nutrient supply. By contrast, the largest gradient in the IPN (weak transfer efficiency) was accompanied by low $\delta^{15}\text{N}_{\text{PN}}$, high N^* and relatively high N

fixation activities. Accordingly, we suggest nitrogen fixation superimposed onto biological fractionation lowers the $\delta^{15}\text{N}_{\text{PN}}$ values in the euphotic zone and weakens the transfer efficiency during periods with shallow MLD due to sluggish sinking of the diazotrophs.

[57] On the other hand, the $\delta^{15}\text{N}$ values of sinking particles collected by sediment trap at depths of 374 and 447 m (mean of 410 m) follow a similar temporal pattern relative to that of $\delta^{15}\text{N}_{\text{PN}}$ in the overlying water column with a lag time of 1 month. The $\delta^{15}\text{N}_{\text{PN}}$ values of trapped material range from 3.3 to 7.3‰ with a flux-weighted mean of 5.6‰, which is slightly deviated from the $\delta^{15}\text{NO}_3$ of the upwelled source. By using a one-dimensional mass and isotope balance model for upper 410 m, we obtained the N fixation input of $\sim 20 \pm 26$ mmol N m⁻² yr⁻¹ under the assumption of steady state and no atmospheric N deposition. This model derived N fixation input accounts for only ~ 5 –10% of the reported new production at SEATS on an annual basis. Similar values of N fixation flux were presented at BATS [Orcutt *et al.*, 2001] and HOTS Station [Karl *et al.*, 1997]. Further investigation on isotopic values are needed for nitrate and sinking PN in subsurface layer at SEATS Station to provide a more reliable estimate. Moreover, the atmospheric deposition could also contribute significant amounts of new N to the ocean [Duce *et al.*, 2008], so a clear demand for future work is the measurement of $\delta^{15}\text{N}$ in order to identify the relative importance of the different N sources to the marine ecosystem.

[58] **Acknowledgments.** Supported by Taiwan (NSC 98-2116-M-001-005, Academia Sinica Thematic Program AFOBI) and China (973 Program, 2009CB421200, and the program of Introducing Talents of Discipline to Universities, B07034).

References

- Altabet, M. A. (1988), Variations in nitrogen isotopic composition between sinking and suspended particles: Implications for nitrogen cycling and particle transformation in the open ocean, *Deep Sea Res., Part A*, 35(4), 535–554, doi:10.1016/0198-0149(88)90130-6.
- Altabet, M. A. (1996), Nitrogen and carbon isotopic tracers of the sources and transformation of particles in the deep sea, in *Particle Flux in the Ocean*, edited by V. Ittekkot *et al.*, pp. 155–184, John Wiley, New York.
- Altabet, M. A., W. G. Deuser, S. Honjo, and C. Stienen (1991), Seasonal and depth-related changes in the source of sinking particles in the North Atlantic, *Nature*, 354, 136–139, doi:10.1038/354136a0.
- Altabet, M. A., M. J. Higginson, and D. W. Murray (2002), The effect of millennial-scale changes in Arabian Sea denitrification on atmospheric CO_2 , *Nature*, 415, 159–162, doi:10.1038/415159a.
- Armstrong, R. A., C. Lee, J. I. Hedges, S. Honjo, and S. G. Wakeham (2002), A new, mechanistic model for organic carbon fluxes in the ocean based on the quantitative association of POC with ballast minerals, *Deep Sea Res., Part II*, 49(1–3), 219–236.
- Bourbonnais, A., M. F. Lehmann, J. J. Waniek, and D. E. Schulz-Bull (2009), Nitrate isotope anomalies reflect N_2 fixation in the Azores Front region (subtropical NE Atlantic), *J. Geophys. Res.*, 114, C03003, doi:10.1029/2007JC004617.
- Capone, D. G., J. P. Zehr, H. W. Paerl, B. Bergman, and E. J. Carpenter (1997), *Trichodesmium*, a globally significant marine cyanobacterium, *Science*, 276, 1221–1229, doi:10.1126/science.276.5316.1221.
- Carpenter, E. J., H. R. Harvey, B. Fry, and D. G. Capone (1997), Biogeochemical tracers of the marine cyanobacterium *Trichodesmium*, *Deep Sea Res Part I*, 44(1), 27–38, doi:10.1016/S0967-0637(96)00091-X.
- Casciotti, K. L., T. W. Trull, D. M. Glover, and D. Davies (2008), Constraints on nitrogen cycling at the subtropical North Pacific Station ALOHA from isotopic measurements of nitrate and particulate nitrogen, *Deep Sea Res., Part II*, 55(14–15), 1661–1672, doi:10.1016/j.dsr2.2008.04.017.
- Chao, S. Y., P. T. Shaw, and S. Y. Wu (1996), El Niño modulation of the South China Sea circulation, *Prog. Oceanogr.*, 38(1), 51–93, doi:10.1016/S0079-6611(96)00010-9.

- Checkley, D. M., Jr., and L. C. Entzeroth (1985), Elemental and isotopic fractionation of carbon and nitrogen by marine, planktonic copepods and implications to the marine nitrogen cycle, *J. Plankton Res.*, 7(4), 553–568, doi:10.1093/plankt/7.4.553.
- Chen, Y. L. (2005), Spatial and seasonal variations of nitrate-based new production and primary production in the South China Sea, *Deep Sea Res., Part I*, 52(2), 319–340, doi:10.1016/j.dsr.2004.11.001.
- Chen, Y. L. L., H. Y. Chen, and Y. H. Lin (2003), Distribution and downward flux of *Trichodesmium* in the South China Sea as influenced by the transport from the Kuroshio Current, *Mar. Ecol. Prog. Ser.*, 259, 47–57, doi:10.3354/meps259047.
- Chen, Y. L. L., H. Y. Chen, S. H. Tuo, and K. Ohki (2008), Seasonal dynamics of new production from *Trichodesmium* N₂ fixation and nitrate uptake in the upstream Kuroshio and South China Sea basin, *Limnol. Oceanogr.*, 53(5), 1705–1721, doi:10.4319/lo.2008.53.5.1705.
- Chou, W. C., Y. L. L. Chen, D. D. Sheu, Y. Y. Shih, C. A. Han, C. L. Cho, C. M. Tseng, and Y. J. Yang (2006), Estimated net community production during the summertime at the SEATS time-series study site, northern South China Sea: Implications for nitrogen fixation, *Geophys. Res. Lett.*, 33, L22610, doi:10.1029/2005GL025365.
- Deutsch, C., N. Gruber, R. M. Key, J. L. Sarmiento, and A. Ganachaud (2001), Denitrification and N₂ fixation in the Pacific Ocean, *Global Biogeochem. Cycles*, 15(2), 483–506, doi:10.1029/2000GB001291.
- Duce, R. A., et al. (2008), Impacts of atmospheric anthropogenic nitrogen on the open ocean, *Science*, 320(5878), 893–897, doi:10.1126/science.1150369.
- Falkowski, P. G. (1997), Evolution of the nitrogen cycle and its influence on the biological sequestration of CO₂ in the ocean, *Nature*, 387, 272–275, doi:10.1038/387272a0.
- Fawcett, S. E., M. W. Lomas, J. R. Casey, B. B. Ward, and D. M. Sigman (2011), Assimilation of upwelled nitrate by small eukaryotes in the Sargasso Sea, *Nat. Geosci.*, 4, 717–722, doi:10.1038/ngeo1265.
- Gaye, B., M. G. Wiesner, and N. Lahajnar (2009), Nitrogen sources in the South China Sea, as discerned from stable nitrogen isotopic ratios in rivers, sinking particles, and sediments, *Mar. Chem.*, 114(3–4), 72–85, doi:10.1016/j.marchem.2009.04.003.
- Hastings, M. G., D. M. Sigman, and F. Lipschultz (2003), Isotopic evidence for source changes of nitrate in rain at Bermuda, *J. Geophys. Res.*, 108(D24), 4790, doi:10.1029/2003JD003789.
- Hsu, S. C., S. C. Liu, Y. T. Huang, S. C. C. Lung, F. Tsai, J. Y. Tu, and S. J. Kao (2008), A criterion for identifying Asian dust events based on Al concentration data collected from northern Taiwan between 2002 and early 2007, *J. Geophys. Res.*, 113, D18306, doi:10.1029/2007JD009574.
- Jia, G. D., and F. J. Chen (2010), Monthly variations in nitrogen isotopes of ammonium and nitrate in wet deposition at Guangzhou, south China, *Atmos. Environ.*, 44(19), 2309–2315, doi:10.1016/j.atmosenv.2010.03.041.
- Kao, S. J., F. K. Shiah, C. H. Wang, and K. K. Liu (2006), Efficient trapping of organic carbon in sediments on the continental margin with high fluvial sediment input off southwestern Taiwan, *Cont. Shelf Res.*, 26(20), 2520–2537, doi:10.1016/j.csr.2006.07.030.
- Karl, D. M., R. Letelier, L. Tupas, J. E. Dore, J. Christian, and D. Hebel (1997), The role of nitrogen fixation in biogeochemical cycling in the subtropical North Pacific Ocean, *Nature*, 388, 533–538, doi:10.1038/41474.
- Kienast, M. (2000), Unchanged nitrogen isotopic composition of organic matter in the South China Sea during the last climatic cycle: Global implications, *Paleoceanography*, 15(2), 244–253, doi:10.1029/1999PA000407.
- Knapp, A. N., D. M. Sigman, and F. Lipschultz (2005), N isotopic composition of dissolved organic nitrogen and nitrate at the Bermuda Atlantic Time-series Study site, *Global Biogeochem. Cycles*, 19, GB1018, doi:10.1029/2004GB002320.
- Knapp, A. N., D. M. Sigman, F. Lipschultz, A. B. Kustka, and D. G. Capone (2011), Interbasin isotopic correspondence between upper-ocean bulk DON and subsurface nitrate and its implications for marine nitrogen cycling, *Global Biogeochem. Cycles*, 25, GB4004, doi:10.1029/2010GB003878.
- Lin, I. I., W. T. Liu, C.-C. Wu, G. T. F. Wong, C. Hu, Z. Q. Chen, W.-D. Liang, Y. Yang, and K.-K. Liu (2003), New evidence for enhanced ocean primary production triggered by tropical cyclone, *Geophys. Res. Lett.*, 30(13), 1718, doi:10.1029/2003GL017141.
- Lin, I.-I., J. P. Chen, G. T. F. Wong, C.-W. Huang, and C.-C. Lien (2007), Aerosol input to the South China Sea: Results from the MODerate Resolution Imaging Spectro-radiometer, the quick scatterometer, and the measurements of pollution in the troposphere sensor, *Deep Sea Res Part II*, 54, 1589–1601, doi:10.1016/j.dsr2.2007.05.013.
- Liu, G., and F. Chai (2009), Seasonal and interannual variability of primary and export production in the South China Sea: A three-dimensional physical–biogeochemical model study, *ICES J. Mar. Sci.*, 66(2), 420–431, doi:10.1093/icesjms/fsn219.
- Liu, H. B., J. Chang, C. M. Tseng, L. S. Wen, and K. K. Liu (2007), Seasonal variability of picoplankton in the northern South China Sea at the SEATS station, *Deep Sea Res., Part II*, 54(14–15), 1602–1616, doi:10.1016/j.dsr2.2007.05.004.
- Liu, K. K., M. J. Su, C. R. Hsueh, and G. C. Gong (1996), The nitrogen isotopic composition of nitrate in the Kuroshio Water northeast of Taiwan: Evidence for nitrogen fixation as a source of isotopically light nitrate, *Mar. Chem.*, 54(3–4), 273–292, doi:10.1016/0304-4203(96)00034-5.
- Liu, K. K., S. Y. Chao, P. T. Shaw, G. C. Gong, C. C. Chen, and T. Y. Tang (2002), Monsoon-forced chlorophyll distribution and primary production in the South China Sea: Observations and a numerical study, *Deep Sea Res., Part I*, 49(8), 1387–1412, doi:10.1016/S0967-0637(02)00035-3.
- Liu, K. K., S. J. Kao, H. C. Hu, W. C. Chou, G. W. Hung, and C. M. Tseng (2007), Carbon isotopic composition of suspended and sinking particulate organic matter in the northern South China Sea: From production to deposition, *Deep Sea Res., Part II*, 54(14–15), 1504–1527, doi:10.1016/j.dsr2.2007.05.010.
- Liu, K. K., C. M. Tseng, C. R. Wu, and I. I. Lin (2010), The South China Sea, in *Carbon and Nutrient Fluxes in Continental Margins: A Global Synthesis*, edited by K. K. Liu et al., pp. 124–146, Springer, Berlin, doi:10.1007/978-3-540-92735-8.
- Loick, N., J. Dippner, H. N. Doan, I. Liskow, and M. Voss (2007), Pelagic nitrogen dynamics in the Vietnamese upwelling area according to stable nitrogen and carbon isotope data, *Deep Sea Res., Part I*, 54(4), 596–607, doi:10.1016/j.dsr.2006.12.009.
- Mahaffey, C., A. F. Michaels, and D. G. Capone (2005), The conundrum of marine nitrogen fixation, *Am. J. Sci.*, 305, 546–595, doi:10.2475/ajs.305.6-8.546.
- Montoya, J. P., C. M. Holl, J. P. Zehr, A. Hansen, T. A. Vilareal, and D. G. Capone (2004), High rates of N₂ fixation by unicellular diazotrophs in the oligotrophic Pacific Ocean, *Nature*, 430, 1027–1032, doi:10.1038/nature02824.
- Mulholland, M. R. (2007), The fate of nitrogen fixed by diazotrophs in the ocean, *Biogeosciences*, 4(1), 37–51, doi:10.5194/bg-4-37-2007.
- Mulholland, M. R., P. W. Bernhardt, C. A. Heil, D. A. Bronk, and J. M. O’Neil (2006), Nitrogen fixation and release of fixed nitrogen by *Trichodesmium* spp. in the Gulf of Mexico, *Limnol. Oceanogr.*, 51(4), 1762–1776, doi:10.4319/lo.2006.51.4.1762.
- O’Neil, J. M., and M. R. Roman (1994), Ingestion of the cyanobacterium *Trichodesmium* spp. by pelagic harpacticoid copepods *Macrosetella*, *Miracia* and *Oculosetella*, *Hydrobiologia*, 292–293(1), 235–240, doi:10.1007/BF00229946.
- O’Neil, J. M., P. M. Metzler, and P. M. Gilbert (1996), Ingestion of ¹⁵N₂-labelled *Trichodesmium* spp and ammonium regeneration by the harpacticoid copepod *Macrosetella gracilis*, *Mar. Biol. Berlin*, 125(1), 89–96, doi:10.1007/BF00350763.
- Orcutt, K. M., F. Lipschultz, K. Gundersen, R. Arimoto, A. F. Michaels, A. H. Knap, and J. R. Gallon (2001), A seasonal study of the significance of N₂ fixation by *Trichodesmium* spp. at the Bermuda Atlantic Time-series Study (BATS) site, *Deep Sea Res., Part II*, 48(8–9), 1583–1608, doi:10.1016/S0967-0645(00)00157-0.
- Qu, T. D., J. B. Girton, and J. A. Whitehead (2006), Deepwater overflow through Luzon Strait, *J. Geophys. Res.*, 111, C01002, doi:10.1029/2005JC003139.
- Saino, T., and A. Hattori (1987), Geographical variation of the water column distribution of suspended particulate organic nitrogen and its ¹⁵N natural abundance in the Pacific and its marginal seas, *Deep Sea Res., Part A*, 34(5–6), 807–827, doi:10.1016/0198-0149(87)90038-0.
- Shaw, P. T. (1991), The seasonal variation of the intrusion of the Philippine Sea water into the South China Sea, *J. Geophys. Res.*, 96(C1), 821–827, doi:10.1029/90JC02367.
- Shiozaki, T., K. Furuya, T. Kodama, S. Kitajima, S. Takeda, T. Takemura, and J. Kanda (2010), New estimation of N₂ fixation in the western and central Pacific Ocean and its marginal seas, *Global Biogeochem. Cycles*, 24, GB1015, doi:10.1029/2009GB003620.
- Sigman, D. M., K. L. Karsh, and K. L. Casciotti (2009), Nitrogen isotopes in the ocean, in *Encyclopedia of Ocean Sciences*, edited by H. S. John, K. T. Karl, and A. T. Steve, pp. 40–54, Academic, Oxford, U. K., doi:10.1016/B978-012374473-9.00632-9.
- Suga, T., K. Motoki, Y. Aoki, and A. M. Macdonald (2004), The North Pacific climatology of winter mixed layer and mode waters, *J. Phys. Oceanogr.*, 34, 3–22, doi:10.1175/1520-0485(2004)034<0003:TNPCCOW>2.0.CO;2.
- Tseng, C. M., G. T. F. Wong, I. I. Lin, C. R. Wu, and K. K. Liu (2005), A unique seasonal pattern in phytoplankton biomass in low-latitude waters

- in the South China Sea, *Geophys. Res. Lett.*, *32*, L08608, doi:10.1029/2004GL022111.
- Voss, M., D. Bombar, N. Loick, and J. W. Dippner (2006), Riverine influence on nitrogen fixation in the upwelling region off Vietnam, South China Sea, *Geophys. Res. Lett.*, *33*, L07604, doi:10.1029/2005GL025569.
- Wong, G. T. F., S.-W. Chung, F.-K. Shiah, C.-C. Chen, L.-S. Wen, and K.-K. Liu (2002), Nitrate anomaly in the upper nutricline in the northern South China Sea—Evidence for nitrogen fixation, *Geophys. Res. Lett.*, *29*(23), 2097, doi:10.1029/2002GL015796.
- Wong, G. T. F., C.-M. Tseng, L.-S. Wen, and S.-W. Chung (2007a), Nutrient dynamics and N-anomaly at the SEATS station, *Deep Sea Res., Part II*, *54*(14–15), 1528–1545, doi:10.1016/j.dsr2.2007.05.011.
- Wong, G. T. F., T.-L. Ku, M. Mulholland, C.-M. Tseng, and D.-P. Wang (2007b), The SouthEast Asian Time-series Study (SEATS) and the biogeochemistry of the South China Sea—An overview, *Deep Sea Res., Part II*, *54*(14–15), 1434–1447, doi:10.1016/j.dsr2.2007.05.012.
- Wu, J. F., S. W. Chung, L. S. Wen, K. K. Liu, Y. L. L. Chen, H. Y. Chen, and D. M. Karl (2003), Dissolved inorganic phosphorus, dissolved iron, and *Trichodesmium* in the oligotrophic South China Sea, *Global Biogeochem. Cycles*, *17*(1), 1008, doi:10.1029/2002GB001924.
- You, Y., C. S. Chern, Y. Yang, C. T. Liu, K. K. Liu, and S. C. Pai (2005), The South China Sea, a cul-de-sac of North Pacific Intermediate Water, *J. Oceanogr.*, *61*, 509–527, doi:10.1007/s10872-005-0059-6.
- Zhang, J., G. S. Zhang, Y. F. Bi, and S. M. Liu (2011), Nitrogen species in rainwater and aerosols of the Yellow and East China seas: Effects of the East Asian monsoon and anthropogenic emissions and relevance for the NW Pacific Ocean, *Global Biogeochem. Cycles*, *25*, GB3020, doi:10.1029/2010GB003896.